




Kondo nanomechanical dissipation in the driven Anderson impurity modelLucas Kohn ¹, Giuseppe E. Santoro,^{1,2,3} Michele Fabrizio,¹ and Erio Tosatti ^{1,2,3}¹*SISSA, Via Bonomea 265, I-34136 Trieste, Italy*²*International Centre for Theoretical Physics, Strada Costiera 11, I-34151 Trieste, Italy*³*CNR-IOM, Via Bonomea 265, I-34136 Trieste, Italy* (Received 13 May 2022; revised 29 November 2022; accepted 3 January 2023; published 17 January 2023)

The cyclic sudden switch of a magnetic impurity from a Kondo to a non-Kondo state and back was recently proposed to involve an important dissipation of the order of several $k_B T_K$ per cycle. The possibility to reveal this and other electronic processes through nanomechanical dissipation by, e.g., ultrasensitive atomic force microscope (AFM) tools would represent an unusual and interesting form of spectroscopy. Here, we explore the dependence on the switching time of the expected dissipation, a quantity whose magnitude is physically expected to drop from maximum to zero between sudden and slow switching, respectively. As an application of a recently established matrix-product-state-based time-dependent variational algorithm, we study the magnetic-field-induced Kondo switching in an Anderson model of the magnetic impurity. We find, quite reasonably, that dissipation requires switching within the Kondo timescale $\hbar(k_B T_K)^{-1}$ or faster. While such a fast switching seems problematic for current AFM setups, the challenge remains open for future means to detect this dissipation by time-dependent magnetic fields, an electrostatic impurity level shift, or hybridization switching. The technical aspects revealed by this approach will be of interest for future nonequilibrium calculations.

DOI: [10.1103/PhysRevB.107.035415](https://doi.org/10.1103/PhysRevB.107.035415)**I. INTRODUCTION**

Interest in the Kondo effect, a paradigmatic single-site many-body phenomenon, has still, 50 years after Anderson's theoretical breakthrough [1,2], not abated. Spectroscopically, zero-bias tunneling anomalies [3] represent the well-known spectroscopic signal of the Kondo effect in electron conductance through a spin-carrying site. More nonequilibrium alternatives are, in principle, provided by nanomechanics. A recent concept is that atomic force microscope (AFM) mechanical dissipation can also serve as a spectroscopic tool, as was shown, for example, with quantum dots [4,5]. The so-called pendulum AFM enables accurate, noninvasive measurements of dissipation in oscillating tip experiments [6–9]. In every cycle, a fraction of the vibrating tip's mechanical energy is dissipated through dynamical processes of all kinds, electronic and magnetic as well as ionic, going on, out of contact, in the sample under the tip. The dissipated energy and its dependence upon parameters such as the strength of interaction between the tip and surface-adsorbed impurity, voltage, temperature, or magnetic field can provide spectroscopic evidence of processes such as the electronic transition in quantum dots and surface unpaired electron centers [4,5], in addition to collective phenomena such as normal-superconductor transitions [7] and structural transitions [9]. Recently, some of us suggested that if the “on-and-off” switching of the Kondo effect could be operated by the tip itself in the course of each oscillation cycle, then a corresponding mechanical dissipation of order $k_B T_K$, where T_K is the Kondo temperature, might be detectable in pendulum AFM measurements [10]. That mechanical cost must be provided to the vibrating tip in order to maintain its oscillation. In that study, the Kondo

switching was modeled by instantaneously turning on and off the hybridization interaction between the impurity and the free electrons in the metal, an approximation that permits us to express the dissipation in terms of equilibrium quantities [10]. A finite-frequency modulation of hybridization was subsequently discussed in Ref. [11], confirming that periodic hybridization switching should contribute a Kondo dissipation per cycle by about $k_B T_K$, without much further ado.

Another possibility to disturb the surface impurity Kondo effect could be just to shift the electronic impurity level from, e.g., well below the Fermi level to near or well above the Fermi level and back again periodically in time. Yet another Kondo switching maneuver could be to expose the impurity to an oscillatory magnetic field. In such hypothetical experiments, however, the on-off Kondo switching does not occur instantaneously—a nonzero mechanical switching time must be required depending on the parameters, including oscillation frequencies, amplitudes, interaction, etc. The Kondo dissipation effect described by Baruselli *et al.* [10] for infinitely fast switching therefore needs to be reconsidered and updated to account for finite switching times, a nonequilibrium calculation which is entirely nontrivial. Here, we choose this problem as a demonstrative application of our recently introduced nonequilibrium approach [12,13]. Our expectation is that a nonzero nonequilibrium dissipation should reasonably require a switching time of the order of $\hbar(k_B T_K)^{-1}$, which is very short compared with the mechanical times of tip-operated systems. In spite of that, a calculation of this type is of interest for its own sake, and we propose it in view of future nonequilibrium applications.

We focus on two separate cases, a time-dependent impurity level shift and a time-dependent magnetic field. For the first, we calculate the dissipation caused by a time-dependent evolution of the impurity energy level, thus modeling the effect of electrostatic tip-impurity interaction on the impurity electronic chemical potential—the mechanism at work in, e.g., Ref. [5]. For the second, we will look for the dissipation effect caused by a time-dependent magnetic field like the one that could be exerted by the stray field of an oscillating ferromagnetic tip.

No dissipation is expected to occur for an infinitely slow, adiabatic, Kondo switching, no matter how the switching is operated, while a sudden, infinitely fast switching of hybridization like that in Ref. [10] would likely provoke the maximum possible dissipation under reasonable assumptions of monotonicity. We should describe how dissipation would drop when the switching velocity is gradually reduced from infinity, where it is largest, to lower and lower values as the switching velocity is reduced.

We address the fundamental quantum mechanical starting point of these questions by simulating the full real-time dynamics of an externally perturbed Anderson model of a quantum impurity whose Kondo effect is switched with different means and time dependences. All results are obtained by employing our recently established, state-of-the-art numerical technique based on matrix product states [12,13].

This paper is organized as follows. Section II summarizes the single-impurity Anderson model, the time-dependent protocol, and the matrix-product-state techniques employed to study the full time dependence of the model. Section III contains the results of our simulations, where dissipation is calculated for the two mechanisms we have considered: a switch of the local impurity level and a switch of a local magnetic field. Finally, Sec. IV contains the final discussion and draws some conclusions.

II. MODEL, PROTOCOL, AND METHOD

A. Anderson model

We shall calculate the dissipated energy in a cycle during which the parameters of a Kondo system are forced to evolve in a time-periodic manner as in an idealized experiment. The Kondo physics is described by the single-impurity Anderson model [14] (SIAM), whose Hamiltonian is

$$\hat{H}_{\text{SIAM}} = \hat{H}_{\text{loc}} + \hat{H}_{\text{hyb}} + \hat{H}_{\text{cond}}. \quad (1)$$

The local term \hat{H}_{loc} describes the impurity and is given by

$$\hat{H}_{\text{loc}} = \sum_{\sigma} \varepsilon_d \hat{d}_{\sigma}^{\dagger} \hat{d}_{\sigma} + U \hat{n}_{\uparrow} \hat{n}_{\downarrow} + B(\hat{n}_{\uparrow} - \hat{n}_{\downarrow}), \quad (2)$$

with an energy level ε_d and on-site Coulomb repulsion U . Additionally, we include a magnetic field B whose Zeeman coupling shifts the energy levels of spin up and spin down in opposite directions. As is well known, the magnetic field destroys the Kondo effect [15,16] and hence provides a control parameter that helps us extract the contribution of the Kondo effect. The impurity couples to conduction electrons through

the hybridization interaction

$$\hat{H}_{\text{hyb}} = \sum_{\sigma} \sum_k V_k (\hat{d}_{\sigma}^{\dagger} \hat{c}_{k\sigma} + \hat{c}_{k\sigma}^{\dagger} \hat{d}_{\sigma}), \quad (3)$$

with spin-independent hybridization couplings V_k . The conduction electrons are, as usual, modeled as a bath of free fermions:

$$\hat{H}_{\text{cond}} = \sum_{\sigma} \sum_k \epsilon_k \hat{c}_{k\sigma}^{\dagger} \hat{c}_{k\sigma}. \quad (4)$$

Without magnetic field, $B = 0$, the model is symmetric under a spin flip and obeys a particle-hole (PH) symmetry if $\varepsilon_d = -U/2$, $V_k = V_{-k}$, $\epsilon_k = -\epsilon_{-k}$. The B field breaks both spin symmetry and PH symmetry, if present. However, at $B \neq 0$ the model is still invariant under the combined PH and spin-flip transformation,

$$\hat{c}_{k,\sigma} \longrightarrow \hat{c}_{-k,-\sigma}^{\dagger}, \quad \hat{d}_{\sigma} \longrightarrow -\hat{d}_{-\sigma}^{\dagger}, \quad (5)$$

provided we make the particle-hole-symmetric choice for U , V_k , and ϵ_k . Throughout this paper we will choose particle-hole-symmetric hybridization energy dependence with a semicircular shape, given by $V^2(x) = \Gamma \sqrt{1-x^2}/\pi W$ in the continuum limit, with hybridization coupling Γ , half bandwidth W , and dimensionless energy $x = \epsilon/W$. Therefore, whereas at zero field the particle-hole symmetry implies $\langle \hat{n}_{\sigma} \rangle = 1/2$ for equilibrium states, in the presence of B we have the lower symmetry $\langle \hat{n}_{\uparrow} + \hat{n}_{\downarrow} \rangle = 1$ for the impurity population.

B. Cyclic dissipation protocol

We consider a time-periodic modulation of the Hamiltonian, to be specified case by case, controlled by a time-dependent control parameter λ , which we assume to follow the time dependence sketched in Fig. 1(a). Hence, a full cycle consists of the following four steps:

(1) The initial Hamiltonian with control parameter $\lambda(t) = \lambda_0$ is kept constant until the system has reached its equilibrium state. This stage describes the tip far away from the impurity.

(2) The control parameter is raised (or lowered) linearly from λ_0 to λ_1 within a time τ , modeling the transient during which the tip approaches and disturbs the impurity.

(3) We let the system relax to its new equilibrium state. That is justified by a relaxation time in this problem expected to be of the order of $\hbar(k_B T_K)^{-1}$, typically much shorter than the time $\tau = (a/A)(2\pi\nu)^{-1}$ during which the tip sweeps near the impurity (\hbar is Planck's constant, a is the impurity lateral size, A is the tip swing amplitude, and ν is the horizontal oscillation frequency).

(4) In the last step, λ turns back to its original value λ_0 in step 1.

In Fig. 1(b) we schematically show the total energy $E(t)$ of the system within a single cycle. During equilibration steps 1 and 3, the total energy is constant, as the Hamiltonian is time independent. In steps 2 and 4, owing to the time dependence of $\lambda = \lambda(t)$, energy is forced to change, and some can be pumped into the system via the impurity—energy can flow from the impurity to or from the bath due to the hybridization coupling. The energy dissipation per cycle E_{diss} is defined as the net energy pumped into the system. It can be calculated as the

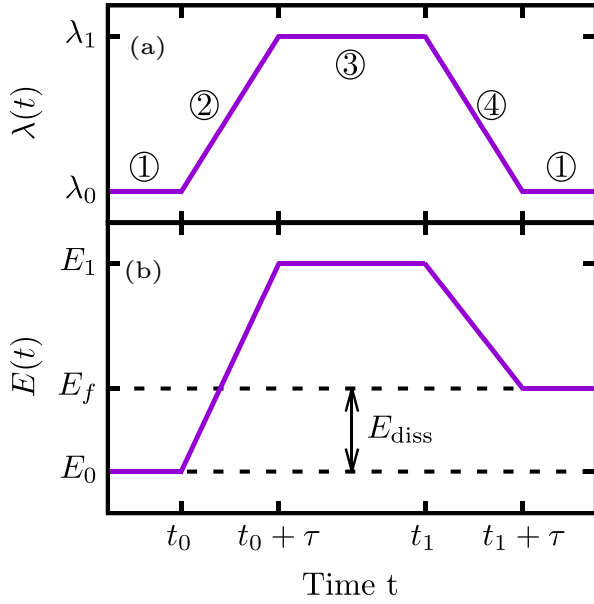


FIG. 1. (a) Time dependence of the driven Hamiltonian parameter λ during a single cycle. In steps 1 and 3 the Hamiltonian is kept constant, and the system equilibrates. In step 2, $\lambda(t)$ changes from $\lambda(t_0) \equiv \lambda_0$ to $\lambda(t_0 + \tau) = \lambda_1$ in a time τ , with linear time dependence. In the last step, step 4, $\lambda(t)$ is brought back from λ_1 to its original value λ_0 . (b) Schematic time evolution of the total energy of the system. The dissipation E_{diss} is given by the energy difference at the beginning and the end of the cycle and is absorbed by the macroscopic bath.

difference between $E_0 = E(t = t_0)$ and $E_f = E(t = t_1 + \tau)$ at the beginning and at the end of the cycle:

$$E_{\text{diss}} = E_f - E_0. \quad (6)$$

One might ask where the energy goes and how a closed system can continuously absorb energy. The answer lies in the macroscopic (infinite) size of the conduction electron bath, which is able to absorb single-site energy without ever heating up. This is particularly easy to exemplify if the bath is represented as a tight-binding chain, with energy being pumped into the impurity and out of it into the bath. Once in the bath, energy can flow away along the chain. Since the chain is infinitely long in the thermodynamic limit, energy never comes back; hence, it is lost forever [17].

Some more practical aspects of the simulation protocol are as follows. In steps 1 and 3, one should theoretically evolve the system until it reaches equilibrium. Because the equilibrium state does not depend on the preceding dynamics, we can carry out steps 1 and 2 and steps 3 and 4 in separate simulations with equilibrium states at times t_0 and t_1 being prepared as the ground states of the corresponding Hamiltonians with control parameters $\lambda(t = t_0)$ and $\lambda(t = t_1)$, respectively. The dissipation is then calculated as

$$E_{\text{diss}} = [E(t_0 + \tau) - E_0] + [E_f - E(t_1)], \quad (7)$$

which simply adds up the energy gains of the system in steps 2 and 4. This is a special formulation of the general

formula in Eq. (6) for the protocol considered in this paper, considering that the system equilibrates in step 3. Notice that this formula reduces to the original definition in Eq. (6) if $E(t_0 + \tau) = E(t_1)$, as is the case when all steps are done in a single run.

C. Quantum evolution method

We compute the dissipation by simulating the full quantum dynamics of the time-dependent Anderson model at zero temperature. In this section, we briefly discuss the mathematical transformations and the technical details to carry out the simulations via matrix product states (MPSs). For more details and the extension to finite temperatures via the so-called *thermofield transformation* [18–21] we refer the reader to Refs. [12,13] and references therein.

The conduction electron bath can be represented in essentially two geometries: (i) The star geometry mimics the geometry of the interactions [see Eq. (3)], where any conduction electron mode interacts with the impurity. In MPS simulations, this geometry requires dealing with long-range interactions but benefits from very low entanglement [22]. The second possible geometry is the chain geometry, where the conduction electrons are mapped into a nearest-neighbor chain [23,24]. This geometry is suitable for tensor network methods because the interactions are only of nearest-neighbor distance, but it suffers from larger entanglement. In this paper, we employ an improved chain mapping of the conduction electrons with *both* short-range interactions and low entanglement [12]. The essential idea of the technique is a separation of electron modes above and below the bath chemical potential, followed by an independent chain mapping. In this way, we avoid the detrimental mixing of filled and empty modes, and we preserve the product state property of the conduction bath's ground state. Mathematically, we define two fermionic operators

$$\hat{a}_{1,0,\sigma} = J_{1,0}^{-1} \sum_{k, \epsilon_k > \mu} V_k \hat{c}_{k,\sigma}, \quad (8)$$

$$\hat{a}_{2,0,\sigma} = J_{2,0}^{-1} \sum_{k, \epsilon_k \leq \mu} V_k \hat{c}_{k,\sigma}, \quad (9)$$

where $J_{c,0}$ ($c = 1, 2$) ensures correct normalization $\{\hat{a}_{c,0,\sigma}, \hat{a}_{c',0,\sigma'}^\dagger\} = \delta_{c,c'} \delta_{\sigma,\sigma'}$. The hybridization term then becomes

$$\hat{H}_{\text{hyb}} = \sum_{\sigma} \sum_{c=1}^2 J_{c,0} (\hat{d}_{\sigma}^\dagger \hat{a}_{c,0,\sigma} + \hat{a}_{c,0,\sigma}^\dagger \hat{d}_{\sigma}). \quad (10)$$

Like in the original chain mapping [23,24], we can apply Lanczos's algorithm independently to $\hat{a}_{1,0,\sigma}$ and $\hat{a}_{2,0,\sigma}$ to obtain two noninteracting chains with fermionic operators $\hat{a}_{c,n,\sigma}$.

In the electron bath ground state, modes with energy above (below) the chemical potential μ are empty (filled). Since $\hat{a}_{1,n,\sigma}$ and $\hat{a}_{2,n,\sigma}$ are linear combinations of modes that are empty (filled) in the ground state, they are completely empty (filled) as well, and hence, the conduction electron bath

ground state is a simple product state, which, as demonstrated in Refs. [12,13], is highly beneficial for the simulations. The

final Hamiltonian to simulate consists of two Wilson's chains and the impurity interacting with the first site of both chains:

$$\hat{H}_{\text{SIAM}}(t) = \hat{H}_{\text{loc}}(t) + \sum_{\sigma} \sum_{c=1}^2 \left\{ J_{c,0} (\hat{d}_{\sigma}^{\dagger} \hat{a}_{c,0,\sigma} + \text{H.c.}) + \sum_{n=0} [E_{c,n} \hat{a}_{c,n,\sigma}^{\dagger} \hat{a}_{c,n,\sigma} + (J_{c,n+1} \hat{a}_{c,n+1,\sigma}^{\dagger} \hat{a}_{c,n,\sigma} + \text{H.c.})] \right\}. \quad (11)$$

Here, the chain coefficients $E_{c,n}$ and $J_{c,n}$ are obtained from the chain mapping. The one-dimensional structure of \hat{H}_{SIAM} together with the short-range nature of interactions allows us to carry out simulations efficiently using matrix product states [25,26]. For equilibrium simulations we employ the density matrix renormalization group (DMRG) algorithm to find ground states [27]. The real-time dynamics of the system with a time-dependent Hamiltonian is computed using the recently developed time-dependent variational principle algorithm in its two-site variant [28], where two neighboring tensors of the MPSs are evolved in time together in each step. This algorithm has proven to deliver very accurate results at low computational costs [29].

At zero temperature, there is one more simplification possible. Instead of calculating the equilibrium state through a preliminary real-time annealing evolution [12], we can simply use the DMRG algorithm to calculate the ground state of the system variationally. Even if finite-temperature simulations are possible as well [12], here, we will, for simplicity, restrict ourselves to zero temperature, where the study of switching-time dependence is more directly addressed.

III. RESULTS

This section describes our results for the dissipation calculated at zero temperature during a cycle where the forcing perturbation varies as in Fig. 1. They should tell us whether or not the dissipation shows signatures of the forced switching of the Kondo effect with two different types of time-periodic cyclic forcing. As anticipated, one consists of a variation of the SIAM impurity energy level periodically up and down across the Fermi level. The second involves the application of

a cyclic magnetic field, varying from zero to a value sufficient to destroy the Kondo effect and back.

A. Time-dependent impurity energy level ε_d

Here, we consider (without or with a static magnetic field B) a time-dependent on-site energy level, taking $\lambda(t) = \varepsilon_d(t)$.

With the protocol discussed above, the impurity energy level is periodically driven between ε_0 and ε_1 , where we choose the particle-hole-symmetric situation $\varepsilon_0 = -U/2$ for the initial state and $\varepsilon_1 = -U/2 + 0.7\Gamma$ for intermediate step 3. The Kondo temperature for $U = 2.5\pi\Gamma$ with PH symmetry is $k_B T_K = 0.07\Gamma$ [12], and hence, the energy level is shifted by $\Delta\varepsilon = \varepsilon_1 - \varepsilon_0 = 0.7\Gamma = 10k_B T_K$.

We start by considering the noninteracting case, $U = 0$. Here, the impurity spectral function has just a single peak (a Friedel resonance), corresponding to the local level of the impurity, broadened due to the hybridization coupling [see Fig. 3(a)]. For a sudden quench ($\tau = 0$) and zero magnetic field ($B = 0$), we find the dissipation $E_{\text{diss}} = 0.29\Gamma$ to be on the order of the level shift $\Delta\varepsilon = 0.7\Gamma$. The dissipation decreases monotonically with increasing magnetic field [see Fig. 2(a)], presumably due to the opposite and compensating effect of the field on the spin-up and spin-down impurity levels. Furthermore, dissipation is reduced by slowing down the time-dependent cycle, as expected, since dissipation must vanish in the limit of an adiabatic evolution.

Let us move next to the interacting case with $U = 2.5\pi\Gamma$ and corresponding Kondo temperature $k_B T_K = 0.07\Gamma$. Again, the impurity level energy is lifted by $\Delta\varepsilon = 0.7\Gamma = 10k_B T_K$. The dissipation turns out to be significantly lower than in the

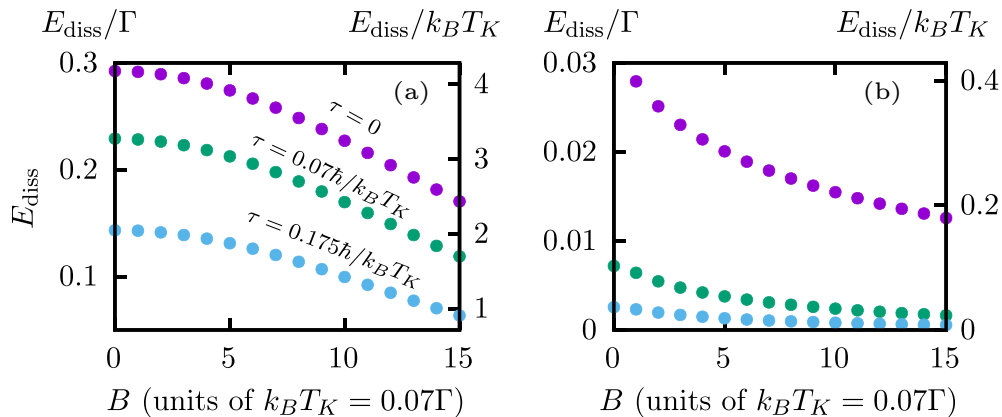


FIG. 2. Dissipation per cycle in (a) the noninteracting case with $U = 0$ and (b) the interacting case with $U = 2.5\pi\Gamma$ at zero temperature for different ramp times τ as a function of the static magnetic field. The impurity level is driven between the particle-hole-symmetric value $\varepsilon_0 = -U/2$ and $\varepsilon_1 = \varepsilon_0 + \Delta\varepsilon$, with $\Delta\varepsilon = 0.7\Gamma = 10k_B T_K$, where the Kondo temperature in the interacting case is $k_B T_K = 0.07\Gamma$. Dissipation is given in units of Γ (left scale) and in units of the Kondo temperature (right scale).

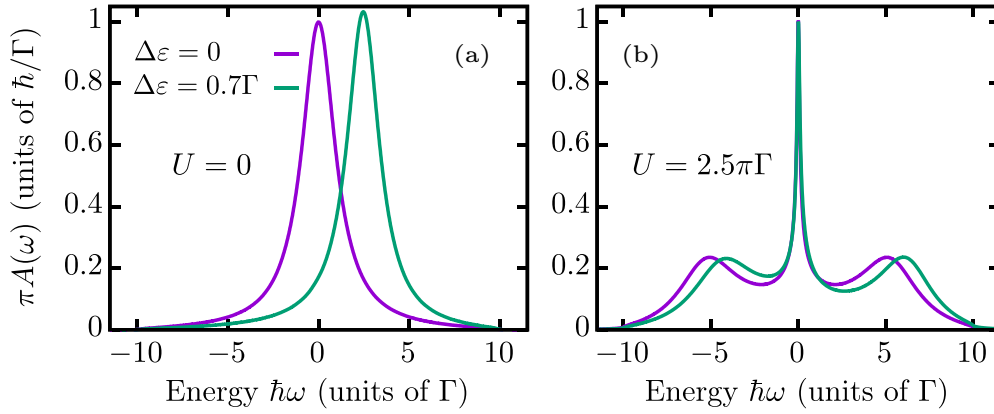


FIG. 3. Zero-temperature equilibrium spectral function in (a) the noninteracting case with $U = 0$ and (b) the interacting case with $U = 2.5\pi\Gamma$, where the latter has Kondo temperature $k_B T_K = 0.07\Gamma$. Two different choices of the impurity energy level $\epsilon_d = -U/2 + \Delta\epsilon$ are considered: the particle-hole-symmetric choice $\Delta\epsilon = 0$ and an asymmetric one with $\Delta\epsilon = 0.7\Gamma$.

noninteracting case, by about one order of magnitude even for the sudden quench (see Fig. 2).

As an incidental note, the magnetic field dependence of the dissipation at $\tau = 0$ follows the (inverse) behavior of the impurity population at ϵ_1 : The occupation is field independent at particle-hole symmetry $\epsilon_d = \epsilon_0$, while dissipation is given by the difference in equilibrium occupations at ϵ_0 and ϵ_1 , which follows immediately from Eq. (7) for a sudden quench of the impurity energy level ϵ_d . The drop in dissipation with increasing ramp time turns out to be very rapid. In fact, the timescale on which dissipation disappears is clearly smaller than the Kondo timescale $\hbar/k_B T_K$, in contrast to what one would expect for the case of dissipation emerging from the Kondo effect. This issue will be discussed in the next section.

To get a better understanding of the mechanisms leading to the observed dissipation, let us analyze the equilibrium impurity spectral function $A(\omega)$, obtained from MPS calculations, as discussed in more detail in Ref. [12]. The noninteracting $U = 0$ spectral function has a single peak due to the local impurity level [see Fig. 3(a)]. The interacting spectral function for $U = 2.5\pi\Gamma$ [see Fig. 3(b)], instead, shows two peaks corresponding to the local impurity levels at $\hbar\omega = \epsilon_d$ and $\hbar\omega = \epsilon_d + U$ and a Kondo peak at the conduction electron Fermi energy, here set to $E_F = 0$. By shifting the impurity energy level from $\Delta\epsilon = 0$ to $\Delta\epsilon = 10k_B T_K$ the two side peaks move accordingly. However, the Kondo peak is barely affected by this impurity level shift. The overall change in the spectral function upon moving the impurity level is much more significant in the noninteracting case, which is clearly the cause of the much larger dissipation but is not of Kondo origin. Summing up this warm-up exercise, a time-dependent chemical potential oscillation shifting the impurity level will not give rise to Kondo dissipation. The physical reason for this, as shown in Fig. 3(b), is that the Kondo peak is barely affected by the perturbation.

In order to cause the Kondo switching electrostatically, the impurity level should be switched in a rather drastic manner, say, from well below $E_F - U$ (doubly occupied impurity, no Kondo effect) to near $E_F - U/2$ (a singly occupied impurity, Kondo regime) or from the latter to well above $E_F + U$ (empty impurity, no Kondo effect). Another perturbation that will lead to Kondo dissipation is, as implemented in Ref. [10],

a periodic on-off switching of impurity-bath hybridization. However, such extreme perturbations will, in real life, be accompanied by an unpredictably large amount of subsidiary dissipation of non-Kondo origin. Therefore, instead of analyzing these cases further, we move directly to the—presumably less dramatic—magnetic switching.

B. Time-dependent magnetic field

We just saw that a gentle electron impurity level switching fails to produce Kondo dissipation because it leaves the narrow Kondo resonance unchanged. On the other hand, an external magnetic field is well known to quench and split the Kondo peak [16,30].

We study the symmetric SIAM ($\epsilon_d = -U/2$) with a time-dependent magnetic field $B(t)$, where B changes between $B_0 = B(t = t_0) = 0$ and $B_1 = B(t_0 + \tau) = 5k_B T_K$. Let us consider in detail the (spin-averaged) spectral function in the presence of a static magnetic field. As shown in Fig. 4, the Kondo peak is essentially gone already at $B = 5k_B T_K$, making

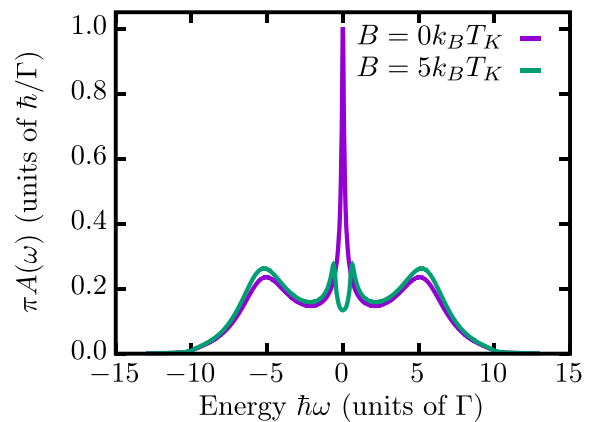


FIG. 4. Spectral function of the SIAM in the absence of a magnetic field, $B = 0$, and for $B = 5k_B T_K$. The model is particle-hole symmetric with $U = 2.5\pi\Gamma$, corresponding to a Kondo temperature of $k_B T_K = 0.07\Gamma$. The spectral function was calculated with the method presented in Ref. [12] and averaged over spin up and spin down (see, e.g., Refs. [30,31]).

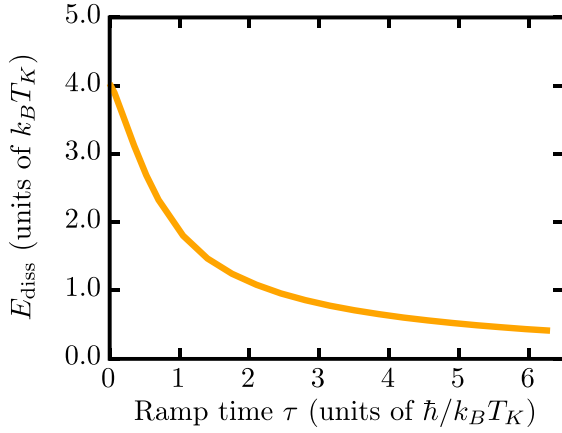


FIG. 5. Dissipation per cycle for the protocol where the magnetic field is linearly changed between $B_0 = 0$ and $B_1 = 5k_B T_K$. The dissipation is on the order of the Kondo temperature and decays on a timescale $t \propto \hbar(k_B T_K)^{-1}$.

the protocol with magnetic field increasing up to $B_1 = 5k_B T_K$ a promising candidate to observe Kondo-related dissipation. Importantly, the local peaks are barely modified by the magnetic field, and hence, we expect only a minor contribution to the dissipation.

Once we make the field B time dependent with the standard on-off protocol in Fig. 1, the dissipation associated with sudden switching of B is, indeed, significantly larger, on the order of $E_{\text{diss}} = 4k_B T_K$, compared to the small dissipation for a time-dependent on-site energy level ε_d . Moreover, as shown by the final result in Fig. 5, the dissipation decays rapidly once the ramp time τ is progressively increased from zero. In fact, the dissipation decays on the timescale of the inverse Kondo temperature, $\hbar(k_B T_K)^{-1}$. A clear rationale is that field variations on larger timescales are felt as essentially adiabatic, causing negligible dissipation. We expect that the very same behavior applies to asymmetric switches of the impurity level energy and to the switching of the hybridization energy considered, in only the sudden limit, by Baruselli *et al.* [10].

IV. DISCUSSION AND CONCLUSIONS

We have confirmed with explicit nonequilibrium calculations that suppression of the Kondo effect by a properly switched magnetic will cause the expected dissipation. A large dissipation, on the order of $E_{\text{diss}} = 4k_B T_K$ per cycle, equal to that originally predicted by Baruselli *et al.* [10], is found when the Kondo switch-off time is sufficiently short, typically $\hbar(k_B T_K)^{-1}$ or shorter. On the contrary, a much smaller dissipation—mostly related to non-Kondo sideband effects in the spectral density—is seen when the impurity level occupation is shifted by similarly large values of the order of $\Delta\varepsilon \sim 10k_B T_K$. It is expected that extremely large energy level oscillations, which we did not try, would present more dissipation through complete destruction of the Kondo effect, but still, it would be hard to discriminate the pure Kondo contribution from others, including the large sideband electronic effects. We instead implemented a time-dependent magnetic field oscillation as a demonstration tool.

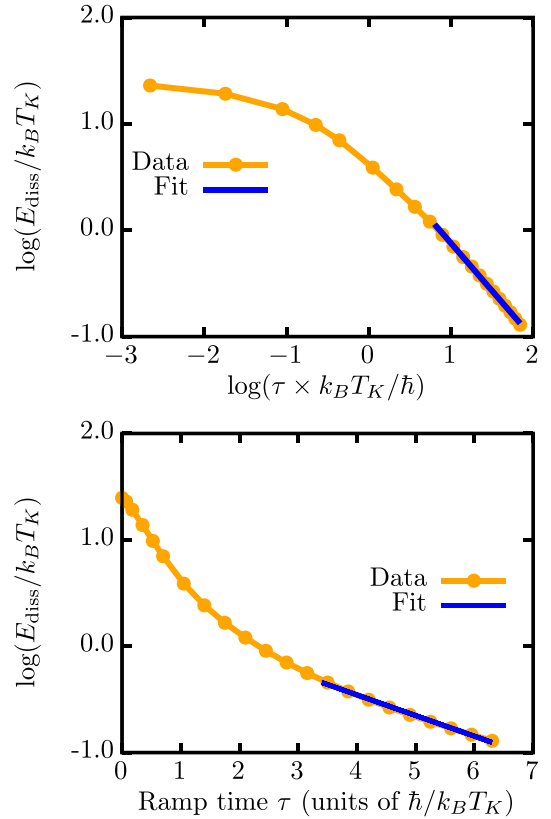


FIG. 6. The dissipation per cycle, as in Fig. 5, versus the ramp time τ in a log-log scale (top) and log-linear scale (bottom). The data are compatible with both a $\tau^{-0.89}$ power law and an exponential decay $\exp(-0.2\tau k_B T/\hbar)$.

Technically, this work represents a nontrivial application of a matrix-product-state-based, time-dependent variational algorithm established by some of us [12,13].

Our result is, as anticipated, that Kondo dissipation drops very quickly with switching time. As Fig. 5 shows, the dissipation drops to about 1/4 of its value once the switching time grows from zero—the sudden switch limit of Ref. [10]—dropping to about $2.5\hbar(k_B T_K)^{-1}$. The simulation times realized are still too short to reveal the asymptotic decay of dissipation as a function of increasing switching times, a decay one should expect to be a power law, controlled by the low-energy behavior and width of the spectral function in Fig. 4. Owing to computational demands, that limit cannot yet be reached, and we must stop at intermediate times. The data in Fig. 6 indicate that the intermediate time decay is compatible with either a $\tau^{-0.89}$ power law or an exponential decay, $\exp(-0.2\tau k_B T/\hbar)$.

The physically short decay times illustrated in Figs. 5 and 6 deny the possibility that the Kondo switching dissipation could be experimentally observed by, e.g., a noncontact pendulum AFM. Consider a tip flying above the surface-deposited Kondo impurity of size a with frequency ν , usually no larger than tens of kilohertz, and large amplitude A , larger than the atomic impurity size $a \sim 0.2$ nm but ordinarily below 10 nm. In the most optimistic case, the tip sway time $a/(A\nu)$ over the impurity, during which the Kondo effect could be switched off and on, could be shrunk

down to perhaps a microsecond, still orders of magnitude longer than $\hbar(k_B T_K)^{-1}$, a time lasting, at most, tens of picoseconds.

In summary, cyclic switching of a magnetic impurity from a Kondo to a non-Kondo state is predicted to involve a very important dissipation on the order of several $k_B T_K$ per cycle. That dissipation critically depends on a sufficiently fast switching time, typically the Kondo time $\hbar(k_B T_K)^{-1}$ or faster. Experimentally, such a fast switching seems problematic for standard AFM setups, but the challenge remains open for other possible means to detect this dissipation by a time-dependent magnetic field, an electrostatic impurity level shift, or hybridization switching. Demonstrating this kind of effect

has represented a nontrivial application of a nonequilibrium quantum evolution method that was recently proposed.

ACKNOWLEDGMENTS

This work was carried out under the European Union's H2020 Framework Programme/ERC Advanced Grant No. 8344023 ULTRADISS. G.E.S. acknowledges that his research has been conducted within the framework of the Trieste Institute for Theoretical Quantum Technologies (TQT). We thank R. Pawlak and E. Meyer (University of Basel) for many helpful discussions. Simulations were performed using the ITENSOR library [32].

-
- [1] P. W. Anderson and G. Yuval, *Phys. Rev. Lett.* **23**, 89 (1969).
 [2] P. W. Anderson, G. Yuval, and D. R. Hamann, *Phys. Rev. B* **1**, 4464 (1970).
 [3] J. A. Appelbaum, *Phys. Rev.* **154**, 633 (1967).
 [4] L. Cockins, Y. Miyahara, S. D. Bennett, A. A. Clerk, S. Studenikin, P. Poole, A. Sachrajda, and P. Grutter, *Proc. Natl. Acad. Sci. USA* **107**, 9496 (2010).
 [5] M. Kisiel, O. O. Brovko, D. Yildiz, R. Pawlak, U. Gysin, E. Tosatti, and E. Meyer, *Nat. Commun.* **9**, 2946 (2018).
 [6] B. Gotsmann, C. Seidel, B. Anczykowski, and H. Fuchs, *Phys. Rev. B* **60**, 11051 (1999).
 [7] M. Kisiel, E. Gnecco, U. Gysin, L. Marot, S. Rast, and E. Meyer, *Nat. Mater.* **10**, 119 (2011).
 [8] M. Langer, M. Kisiel, R. Pawlak, F. Pellegrini, G. E. Santoro, R. Buzio, A. Gerbi, G. Balakrishnan, A. Baratoff, E. Tosatti, and E. Meyer, *Nat. Mater.* **13**, 173 (2014).
 [9] M. Kisiel, F. Pellegrini, G. E. Santoro, M. Samadashvili, R. Pawlak, A. Benassi, U. Gysin, R. Buzio, A. Gerbi, E. Meyer, and E. Tosatti, *Phys. Rev. Lett.* **115**, 046101 (2015).
 [10] P. P. Baruselli, M. Fabrizio, and E. Tosatti, *Phys. Rev. B* **96**, 075113 (2017).
 [11] P. P. Baruselli and E. Tosatti, [arXiv:1804.04999](https://arxiv.org/abs/1804.04999).
 [12] L. Kohn and G. E. Santoro, *Phys. Rev. B* **104**, 014303 (2021).
 [13] L. Kohn and G. E. Santoro, *J. Stat. Mech.* (2022) 063102.
 [14] P. W. Anderson, *Phys. Rev.* **124**, 41 (1961).
 [15] A. C. Hewson, *The Kondo Problem to Heavy Fermions* (Cambridge University Press, Cambridge, 1997).
 [16] T. A. Costi, *Phys. Rev. Lett.* **85**, 1504 (2000).
 [17] A. W. Chin, Á. Rivas, S. F. Huelga, and M. B. Plenio, *J. Math. Phys.* **51**, 092109 (2010).
 [18] Y. Takahashi and H. Umezawa, *Collect. Phenom.* **2**, 55 (1975).
 [19] I. de Vega and M.-C. Bañuls, *Phys. Rev. A* **92**, 052116 (2015).
 [20] F. Schwarz, I. Weymann, J. von Delft, and A. Weichselbaum, *Phys. Rev. Lett.* **121**, 137702 (2018).
 [21] A. Nüßeler, I. Dhand, S. F. Huelga, and M. B. Plenio, *Phys. Rev. B* **101**, 155134 (2020).
 [22] F. A. Wolf, I. P. McCulloch, and U. Schollwöck, *Phys. Rev. B* **90**, 235131 (2014).
 [23] K. G. Wilson, *Rev. Mod. Phys.* **47**, 773 (1975).
 [24] R. Bulla, T. A. Costi, and T. Pruschke, *Rev. Mod. Phys.* **80**, 395 (2008).
 [25] U. Schollwöck, *Rev. Mod. Phys.* **77**, 259 (2005).
 [26] U. Schollwöck, *Ann. Phys. (NY)* **326**, 96 (2011).
 [27] S. R. White, *Phys. Rev. Lett.* **69**, 2863 (1992).
 [28] J. Haegeman, C. Lubich, I. Oseledets, B. Vandereycken, and F. Verstraete, *Phys. Rev. B* **94**, 165116 (2016).
 [29] S. Paeckel, T. Köhler, A. Swoboda, S. R. Manmana, U. Schollwöck, and C. Hubig, *Ann. Phys. (NY)* **411**, 167998 (2019).
 [30] D. M. Fugger, A. Dorda, F. Schwarz, J. von Delft, and E. Arrigoni, *New J. Phys.* **20**, 013030 (2018).
 [31] R. Žitko and T. Pruschke, *New J. Phys.* **12**, 063040 (2010).
 [32] M. Fishman, S. R. White, and E. M. Stoudenmire, *SciPost Phys. Codebases* **4** (2022).